Extracellular matrix-derived hydrogels for dental stem cell delivery

Journal Item

EXTRACELLULAR MATRIX-DERIVED HYDROGELS FOR DENTAL STEM CELL DELIVERY

No benefit of any kind will be received either directly or indirectly by the author(s).

Aiswarya Viswanath [a, c, 1], Julie Vanacker [a, 1], Loïc Germain [a], Julian G Leprince [a], Anibal. Diogenes [b], Kevin Shakesheff [c], Lisa J White [c, 1], Anne des Rieux [a, 1*]

[a] Louvain Drug Research Institute, Advanced Drug Delivery and Biomaterials Unit, Université Catholique de Louvain, Brussels, Belgium.

[b] Department of Endodontics, University of Texas Health Science Center at San Antonio, San Antonio-TX, USA

[c] School of Pharmacy, University of Nottingham, Nottingham NG7 2RD, UK

[1] These authors contributed equally.

[*] Corresponding author: Anne des Rieux, anne.desrieux@uclouvain.be

Abstract

Decellularised mammalian extracellular matrices (ECM) have been widely accepted as an ideal substrate for repair and remodelling of numerous tissues in clinical and pre-clinical studies. Recent studies have demonstrated the ability of ECM scaffolds derived from site-specific homologous tissues to direct cell differentiation. The present study investigated the suitability of hydrogels derived from different source tissues: bone, spinal cord and dentine, as suitable carriers to deliver human apical papilla derived mesenchymal stem cells (SCAP) for spinal cord regeneration. Bone, spinal cord and dentine ECM hydrogels exhibited distinct structural, mechanical and biological characteristics. All three hydrogels supported SCAP viability and proliferation. However, only spinal cord and bone derived hydrogels promoted the expression of neural lineage markers. The specific environment of ECM scaffolds significantly affected the differentiation of SCAP to a neural lineage, with stronger responses observed with spinal cord ECM hydrogels, suggesting that site-specific tissues are more likely to facilitate optimal stem cell behaviour for constructive spinal cord regeneration.

Key words

ECM hydrogels, Dental stem cell delivery, Spinal cord, Bone, Dentine

1 Introduction

Traumatic spinal cord injuries (SCI) cause devastating neurological deficits and disabilities. Initial trauma leads to immediate disruption of neural tissue by axon shearing, blood vessel rupture and cell death. Subsequently a cascade of secondary events occurs composed of ischemic injury, inflammation, cell death, demyelination of axonal tracts and the creation of a glial scar, forming a physical and chemical barrier [1]. Treatment options for SCI have been limited in part due to this complex pathophysiology [2]. Cell transplantation to replace damaged cells, provide trophic support and promote functional recovery is a favourable strategy for SCI [3].

Stem cells derived from dental tissues are an attractive source for cell transplantation in the central nervous system (CNS) due to accessible supply, high proliferation rate and the potential for autologous transplantation [4]. Human dental stem cells are of neural crest origin, display neural stem cell properties [5], and have recently been shown to induce functional recovery in SCI repair [6]. Whilst several different populations of dental stem cells have been identified, stem cells of the apical papilla (SCAP) have been shown to possess greater proliferation potential than dental pulp stem cells [7] and express a variety of neural markers including βIII tubulin, NeuN, nestin, neurofilament M and glial fibrillary acidic protein (GFAP) [5,8]. Recently, whole human apical papillae implanted into rat hemisected spinal cords induced a significant improvement of rat motor function [4]. However, SCAP cells transplanted in a fibrin hydrogel in the same study did not have the same effect upon motor function [4], highlighting the importance of delivering SCAPs in their original niche or a similarly supportive medium. The goal of the present work was thus to identify a suitable hydrogel to support SCAP delivery for SCI.

Biologic scaffolds composed of extracellular matrix (ECM) produced by decellularisation of mammalian tissues largely retain the functional complexity of their tissues of origin [9]. Hydrogel forms of ECM do not retain the three dimensional ultrastructure of the native tissue but still maintain *in vitro* and *in vivo* biologic activity, including differentiation stimuli for neural stem cells [9,10] and the promotion of an M2 macrophage phenotype [11,12]. In addition, ECM hydrogels may supply signalling molecules and growth factors [13,14] required to support delivered cells in the CNS [15]. Tissue-specific ECM scaffolds, originating from a tissue type

homologous to the repair site, have previously shown the ability to enhance site appropriate cell phenotypes compared to ECM scaffolds derived from non-homologous tissues for a range of complex tissues [16-18].

The objectives of the present study were to evaluate the suitability of different ECM derived hydrogels to support SCAPs for delivery into SCI. Previously developed protocols were utilised to produce bone and spinal cord ECM hydrogels (bECMh and scECMh, respectively) and a new method was developed to create a hydrogel form of human dentine ECM (dECMh). The biomolecular composition, mechanical properties, and *in vitro* cytocompatibility of the hydrogels were evaluated. We hypothesised that the different ECM hydrogels would influence SCAP viability, proliferation and gene expression.

2 Material and methods

2.1 Chemicals and reagents

The Quant-iT™ Picogreen® assay kit and the Presto Blue kit were from Life Technologies (Carlsbad, US). Bovine serum, L-glutamine, penicillin and streptomycin were from Gemini Bio-Products (Sera Laboratories International, Bolney, UK). All other reagents were purchased from Sigma-Aldrich (Poole, UK).

2.2 ECM biologic scaffold production

Porcine spinal cord and bovine bone were obtained from market weight animals. Human wisdom teeth were collected from healthy individuals aged between 16 and 18 years. An informed consent was obtained from all donors (Approved by the Commission d'Ethique Biomédicale Hospitalo-Facultaire of UCL, 2012/14JUN/283). Female and male donors and animals have been used indiscriminately. Decellularisation of bone (bECM) [19] and spinal cord (scECM) [20] were performed as described previously. Extraction of ECM from human dentine (dECM) was performed using the protocol developed for bECM preparation with modifications. Briefly, teeth were frozen in liquid nitrogen and broken with a Carver press (Carver, #3850, Wabash, US) and the pulp was removed. The enamel was destroyed by sonication in 10% HCl for 20 min [21]. Acid neutralisation was performed by immersing the tissue in 2 volumes of water containing penicillin-streptomycin (0.5% w/v) for 1 hr. Demineralisation was performed by incubating tooth fragments in a 0.5M HCl solution under agitation (300 rpm) for 24 hrs at room temperature. The resultant material was washed thoroughly with deionised water

and incubated in a 0.05% trypsin-0.025% EDTA solution for 24 hrs at 37˚C at 300rpm for enzymatic decellularisation. Finally, the material was washed with 2 volumes of PBS and freeze dried.

2.3 ECM digestion and solubilisation

Pepsin digestion and solubilisation was used to obtained pre-gel solutions [22,23]. Lyophilised ECM powders were added to 1mg/ml of pepsin in 0.01 N HCl for a final concentration of 10 mg ECM/ml. The suspension was stirred at room temperature for 48 hrs for spinal cord ECM, 72 hrs for dentine ECM and 84 hrs for bone ECM. The resultant pepsin digests were aliquoted and stored at -20^{0}C. Gelation of pepsin digests was induced by neutralisation of salt concentration and pH at 4°C followed by warming to 37˚C. Briefly, pepsin digests were mixed with one tenth volume of 0.01N NaOH, one ninth volume of 10X PBS and made up to desired volume with 1X PBS. 8 mg/ml of pre-gel solutions were prepared and incubated for 1 hr at 37°C to obtain spinal cord, bone and dentine hydrogels, denoted scECMh, bECMh and dECMh.

2.4 DNA, collagen and sGAG quantification

Quantitative assessment of DNA in pepsin digests was conducted by an adaptation of previously published method [23]. DNA was extracted from pepsin digests by addition of an equal volume of 25:24:1 (v:v:v) phenol/chloroform/isoamyl to 1ml of sample (10 mg/ml). Phenol was removed using an equal volume of 24:1 (v:v) chloroform/isoamyl alcohol. DNA was precipitated from the aqueous phase by the addition of 2 volumes of ice-cold ethanol and 0.1 volume of 3M sodium acetate (pH 5.2) and was frozen at -80^{0}C for 30 min. The frozen DNA was then centrifuged at 13,000 rpm for 10 min and washed with ethanol, dried at room temperature and resuspended in 0.1 ml of TE buffer. DNA concentration was measured using a Quant-iT™ Picogreen® assay kit following supplier instructions. A standard curve was prepared with known DNA concentrations from 0 – 100 ng/ml and samples were read using a Tecan Infinite M200 plate reader (Tecan UK, Reading, UK).

Collagen content of pepsin digests was measured by quantifying hydroxyproline [24]. Briefly, pepsin digests and a blank pepsin solution were hydrolysed with 1 volume of concentrated HCl (12N) overnight at 120˚C. The samples were dried by incubation at 90˚C for 2 hrs followed by the addition of 4 volumes of 0.25 M sodium phosphate buffer (pH 6.5). The hydrolysed blank pepsin solution served as a negative control as well as diluent

for the assay. The samples were oxidised by incubation with 1 volume of 3-Chloramine T solution (0.07M) at room temperature for 20 min followed by the addition of 4- *p*-dimethylaminobenzaldehyde (*p*-DAB) solution [1.16M *p*-DAB in 60% perchloric acid (6.5ml) and Isopropanol (15ml)] and incubation at 60^0C for 30 min. A standard curve was prepared using known concentrations of hydroxyproline ranging from 0 – 100 µg/ml and the absorbance was measured at 540nm with a Tecan Infinite M200 plate reader. Collagen content was determined using the relationship that hydroxyproline forms 14.3% of total amount of collagen [24].

The sulphated glycosaminoglycan (sGAG) content in pepsin digests was determined using the 1, 9–Dimethyl methylene blue assay (DMMB) [25]. One ml of digest was incubated with 0.1mg/ml of Proteinase K (>600U/ml) overnight at 37˚C. A solution of blank pepsin was used as negative control as well as diluent for the assay. 50µl of sample was mixed with 200 µl of DMMB solution (0.03 M sodium formate, 0.046M DMMB, ethanol (0.5% v/v) and formic acid (0.2% v/v) in a 96 well plate. A standard curve was constructed using known concentrations of Chondroitin-4-sulphate from 0 – 75 µg/ml. The absorbance was measured immediately at 525nm.

2.5 ECM-based hydrogel gelation kinetics

Turbidimetric gelation kinetics of ECM-based hydrogels was determined as previously described [26]. Normalised Absorbance (NA) was calculated as shown in Eq. (1).

$$NA = \frac{A - A0}{Amax - Ao} \quad (1)$$

Were A is absorbance at given time, A_0 is the initial absorbance and A_{max} is the maximum absorbance attained by the sample after inducing gelation. Normalised gelation was used to calculate the time at which 50% of gelation ($t_{1/2}$) and 95% of gelation (t_{95}) occurred. The lag time, t_{lag}, was defined as the intercept of the linear region of the gelation with 0% absorbance [19]. Speed of gelation (*S*) was determined by calculating the slope of the curve (n=8).

2.6 Rheological characteristics

bECMh, dECMh, and scECMh rheological characteristics were determined as described previously [19] using a Malvern Kinexus ultra+ rheometer (Malvern Kinexus Pro rotational rheometer and rSpace software, Malvern

Instruments, Worcestershire, UK). Cold pre-gel solutions were placed between two pre-cooled (4°C) 25 mm parallel plates separated by a gap of 0.3 mm. For each run, the plates were warmed to reach 37°C (2°C/sec) and the sample was exposed to 1% oscillatory strain with a constant angular frequency of 2 rad/sec. Data were recorded every 30 sec (n=3).

2.7 Scanning electron microscopy (SEM)

Gel specimens (300 µl per well) were fixed in 5 % glutaraldehyde at room temperature. Samples were dehydrated in a graded series of ethanol (25-100%), dried using a critical point dryer (CPD, Balzers Union, Balzers, FL) and sputter coated with gold using a Cressington 208HR metalizer (ELOISE s.a.r.l., Tremblay, FR). Images were acquired using a JSM-7600F (JEOL, Zaventem, BE) scanning electron microscope at a voltage of 15 kV.

2.8 SCAP culture

Previously characterised human stem cells of the apical papilla (SCAP) (RP89 cells) [27] were used between passages 6 and 9. SCAP were grown at 37°C in 5% CO_2 in Minimum Essential Medium (Sigma-Aldrich) supplemented by 10% bovine serum (Gemini Bio-Products), 1% of L-glutamine (Gemini) and 1% of penicillin and streptomycin (Gemini) until they reached ~80% confluence. SCAP were then incorporated in the pre-gel solutions, placed in 96 well plates and incubated at 37°C for 1 hr.

2.9 SCAP viability

Pre- gel solution (10µl) containing 500,000 cells/ml were loaded into µ-Slide Angiogenesis ibiTreat microscopy chamber (Ibidi, Proxylab, Beloeil, BE) and were allowed to gel (n=3, N=3). After 2 days, a Live/Dead assay was performed. Pictures (2 fields/sample, Z-stack: 1 picture every 3µm, for a total of 210 pictures/stack) were then acquired with a confocal microscope (LSM700, Zeiss, Zaventem, BE). All the pictures were merged to count dead and living cells. Cell viability was expressed as a percentage of the number of living cells compared to the total number of cells.

2.10 SCAP proliferation

The effect of ECM origin on SCAP proliferation was analysed when cells were encapsulated in the hydrogels (3D culture) or grown on the surface of hydrogel (2D culture).

2.10.1 SCAP proliferation in 3D culture

Pre-gel solutions containing 500,000 SCAP/ml were placed in 96 well plates (N=3, n=6) and incubated for 1hr at 37°C to initiate gel formation. Pre-gel solution (100µl) without cells was used as a control. Independent samples were prepared for each time point. After 2, 7 and 14 days, cell proliferation was analysed using a Presto Blue kit. The fluorescence intensities (590 nm) were measured 2 hours after the addition of the Presto Blue reagent. Values obtained for hydrogels without cells were used as background and subtracted from values obtained for hydrogels with cells. A standard curve (from 13,000 to 250,000 cells) was used to correlate the fluorescence intensity with cell number. Cell number fold increase was calculated by dividing the number of cells at day 2, 7 or 14 by the initial number of seeded cells. Samples were collected and frozen at -80°C for further processing for PCR analysis.

2.10.2 SCAP proliferation in 2D culture

Pre-gel solutions (20µl) were placed in 96 well plates and allowed to gel for 1 hr at 37°C. Two thousands cells were seeded onto the surface of the hydrogels (N=3, n=6). Cell proliferation was evaluated as described for 2.10.1.

2.11 SCAP gene expression

Total mRNA was extracted using the phenol/chloroform extraction method. One microgram of mRNA was reverse transcribed using the Reverse Transcription System kit (Promega, Madison, USA) (n=3). The resulting cDNA was used as template for 30 cycles of semi-quantitative polymerase chain reaction in a T100 TM thermo cycler (Bio-Rad, BE). Primer sequences are summarized in Table 1. The PCR products were pooled and subjected to electrophoresis on Syber™Safe (Invitrogen, BE) stained 2% agarose gel. mRNA relative expression of tested genes was normalised with GAPDH.

2.12 Statistical analysis

Statistical analyses were performed using PRISM (GraphPad software, CA, USA) and JMP10 (SAS, NC, USA). Two-way ANOVA with post hoc Bonferroni's multiple comparison tests as well as Tukey's HSD were performed with a P-value of 0.05. Errors bars represent the standard deviation (SD) in all figures.

3 Results

3.1 Influence of ECM origin on cellular, collagen and sGAG content

Determination of decellularisation efficiency was based upon quantification of dsDNA. Regardless of origin, all three ECMs contained less than 50 ng/mg of dsDNA (Figure 1A). Concentrations of nucleic acid of bECM, dECM and scECM were significantly different with the lowest quantity detected in scECM; bECM, dECM and scECM contained 17.8±1.5 ng of DNA/mg, 13.56±0.5 ng of DNA/mg and 6.8±0.17 ng of DNA/mg, respectively. No significant difference was observed between the collagen content of the three ECMs, although scECM tended to contain less collagen (Figure 1B); bECM, dECM and scECM contained 84.28±10.20 %, 83.16±5.55 % and 67.41±23.16 % of collagen, respectively. Significantly more sGAG was detected in scECM (0.65 % of dry weight) compared to bECM and dECM (0.3 % and 0%, respectively) (Figure 1C).

3.2 Influence of ECM origin on hydrogel gelation kinetics

The gelation kinetics of scECMh, bECMh and dECMh were sigmoidal, and gelation occurred within 40 min (Figure 2). The t_{lag} and $t_{1/2}$ was 1.40-1.53 fold lower for dECMh compared to sc ECMh and bECMh. However, the time required to reach 95% of the final turbidity is 0.75-0.84 fold lower for scECMh with respect to bECMh and dECMh. The gelation speed was 1.3 and 2.1 fold faster for scECMh compared to bECMh, dECMh respectively (Table 2).

3.3 Influence of ECM origin on hydrogel mechanical properties

Storage modulus (G') and loss modulus (G'') of all the pre-gel solutions increased 5 min after pH neutralisation and temperature elevation and reached a maximum after 1 hr (Figure 3). G' was consistently higher than G", reflecting the formation of a solid hydrogel. Regardless of origin, hydrogels showed similar gelation profiles, although bECMh, dECMh and scECMh final moduli were significantly different (Table 3). bECMh had the

highest storage modulus (287.17 +/- 8.43 Pa); while scECMh and dECMh were significantly lower (19.35 +/- 1.16 and 4.79 +/- 0.33 Pa, respectively).

3.4 Influence of ECM origin on hydrogel microstructure

The origin of hydrogel markedly influenced the hydrogel morphology. While bECMh and dECMh exhibited a fibrillary structure with disorganised thin fibres (Figure 4A and B); scECMh showed a honeycomb structure with thick walls and large pores (Figure 4C). dECMh appeared to be composed of thicker fibres and smaller pores in comparison to bECMh.

3.5 Influence of ECM origin on dental stem cell proliferation

Regardless of the ECM origin, SCAP proliferated when incorporated in the ECM hydrogels. When cultured in 3D, the number of SCAP increased between 0.36 and 1.47-fold 7 days post seeding and 2 to 4.78-fold 14 days post seeding compared to the initial seeding density (Figure 5A). No significant difference was observed between day 2 and 7 for any of the hydrogels, whilst SCAP proliferation significantly increased between day 7 and day 14 for all of the hydrogels. The SCAP proliferation was 1.8 to 2.5-fold higher in scECMh compared to the dECMh and bECMh on day 14, respectively.

When grown on the hydrogels (2D culture), the SCAP proliferation on various ECM hydrogels increased between 0.48 to 1-fold 7 days of post seeding and between 12.6 to 60-folds 14 days post seeding (Figure 5B). SCAP proliferation on tissue culture treated plastic (TCP) was much higher than either on 2D or in 3D hydrogels with a fold increases of 16.28 and 205.7 at day 7 and 14, respectively. No significant difference was observed between Day 2 and 7.

3.6 Influence of SCAP incorporation into different ECM on cell viability

SCAP viability 2 days after incorporation in all ECM hydrogels was above 65 % (Figure 6B). Viability was significantly higher in bECMh than in dECMh and scECMh (85 %, 65 % and 68 %, respectively). In general, SCAP morphology was elongated in all three ECM hydrogels, however some rounded cells were also observed in bECMh (Figure 6A).

3.7 Influence of ECM origin on SCAP gene expression

The expression of genes related to the neural lineage (SNAIL, βIIITubulin, GDNF, VEGFA, PDGFRa, and GAPDH as a housekeeping gene) were analysed to determine whether ECM origin would elicit or support SCAP orientation. When SCAP were cultured routinely (Figure 7), GDNF and PDGFRa were slightly expressed but no expression of SNAIL, βIIITubulin or VEGFA was detected. When SCAP were incorporated in bECM, no expression of the gene of interest was detected at Day 2 and Day 7. SNAIL, βIIITubulin, GDNF, VEGFA and PDGFRa were expressed after 14 days of incubation in the hydrogel. SCAP incorporated in dECM showed no expression of the genes of interest. Only when SCAP were grown in scECM a marked expression of all the tested genes was detected after 7 days.

4 Discussion

The present study illustrates the influence of biological scaffolds derived from homologous and non-homologous tissue on the gene expression profile of dental stem cells from apical papilla (SCAP). Previously published methods were employed to prepare ECM scaffolds derived from spinal cord (scECM) [20] and bone (bECM) [19]. A new decellularisation method was developed for the preparation of dentine ECM scaffolds (dECM) based on the material characteristics and its similarity towards the bone tissue.

The acellular nature of bECM, dECM, and scECM was determined by quantifying residual dsDNA content. The amount of dsDNA per mg of dry ECM present in bECM, dECM and scECM was considerably lower than the <50 ng threshold previously determined as an effective criteria for decellularisation [28]. The presence of DNA and other cellular material, either xenogeneic or allogeneic in nature, within in the ECM scaffold due to inefficient decellularisation could potentially elicit host immunological response. However, it is unlikely that complete removal of cells will be obtained even with harsh decellularisation procedures [29].

The percentage of collagen and glycosaminoglycan in the ECM scaffolds derived from bone, spinal cord and dentine varied depending upon the function and nature of tissue source. In addition to the intrinsic ECM composition influencing sGAG content, the higher sGAG content in scECMh could be due to the decellularisation process. It has been demonstrated previously that small intestinal mucosa-based ECM matrix

sterilised with peracetic acid induced a greater loss of cellular components such as lipids, nucleic acids, and other undesirable elements ensuing more sGAG and FGF-2 compared to ECM non-treated with peracetic acid. We postulate that the higher sGAG content in scECM with respect to bECM and dECM might be due to the peracetic acid treatment during decellularization[30]. Also, we hypothesize that the differences observed between ECM of different origins might be due to i) either different amounts of sGAG in the tissue before treatment or ii) to the different treatments used to obtain each ECM[30,31].

The gelation kinetics based on turbidimetry demonstrated that scECM, bECM and dECM hydrogels (Figure 2) exhibited sigmoidal gelation kinetics. Although the speed to complete gelation as well as t_{95} were greater for scECMh and bECMh, the lag time as well as $t_{1/2}$ of dECMh was considerably lower with respect to bECMh; this is likely to be the effect of glycosaminoglycan presence during the *in vitro* self-assembly of collagen fibres[32].

It is noteworthy that the individual ECMs demonstrate distinct morphologies when analysed via scanning electron microscopy. The basal lamina of the spinal cord is comprised predominantly of collagen IV though types I and III are also present [33] whereas bone and dentine are composed primarily of collagen type I, with traces of type III, V, IX, XII, XIV, XIX, and XXI [34]. We hypothesise that scECMh contains Type IV collagen that tends to form a flexible triple helix that self-assembles to incorporate structural glycoproteins [35], resulting in the sheet-like structure observed in Figure 4C. However in bECMh and dECMh collagen XII, XIV, XIX, and XXI serve as molecular bridges between collagen I monomers to produce fibrils.

Rheology was used to study the viscoelastic properties of ECM hydrogels. It is interesting to note that regardless of the tissue origin, hydrogels exhibited similar sigmoidal shaped gelation profiles. However, the storage modulus for dECMh is considerably lower than scECMh and bECMh. We postulate that this difference is due to the disparity of source of tissue as well as the decellularisation processes. The potential impact of hydrogel solid content has been evaluated but no difference was visible between hydrogels of different origins (Supplementary data 2). We hypothesize that the degree of cross-linking could be responsible for the difference

of moduli, especially when considering the different morphologies observed with SEM[36,37]. Although the final moduli of dECM and scECM are lower than 0.1kPa, the final modulus of bECMh was in the range of 0.1-1.0kPa. Hydrogels with elastic moduli within this range have been reported to have a positive influence on the probability of neuronal marker expression and neuronal differentiation[38].

Several authors have emphasised the intrinsic ability of ECM derived scaffolds to aid viability, migration and proliferation of numerous cell types [9,39]. Nevertheless, the present study is the first time ECM scaffolds from decellularised bone, dentine and spinal cord have been used as a 3D culture system for apical papilla stem cells. High cell viability (Figure 6) was observed in bECMh, scECMh and dECMh, confirming the suitability of these scaffolds as delivery vehicles for SCAP. Greater cell viability was observed in bECMh compared to dECMh and scECMh. The choice of detergents used for the decellularisation procedure could have a marked deleterious effect up on the ECM [40]. We hypothesise that the lower cell viability observed in scECMh may be due to traces of residual detergent present after decellularisation. This is the first time that dentine has been decellularised and further studies may be needed to optimise the duration as well as the concentration of HCl solution used in the enamel removal step. We postulate that too harsh treatment applied during decellularisation procedure may have led to the lower cell viability observed in dECMh

In both 2D and 3D culture environment, SCAP proliferated till day 7 irrespective of the culture conditions (Figure 5). However, in the 2D environment, there was a remarkable increase in the proliferation between day 7 and day 14 for SCAP grown on TCP and dECMh. We postulate that after the initial phase of cell and ECM hydrogel interaction, the surface with higher elasticity (dECMh) facilitated quicker cell migration and proliferation compared to the more rigid surfaces of bECMh and scECMh. SCAP grown in 2D culture proliferated faster than SCAP grown in 3D. Cell movement on 2D environment is relatively unrestricted; whereas in a 3D environment, cells need to degrade their adjacent material enzymatically in order to migrate [41]. Furthermore, in 2D culture, the cells are exposed to a homogenous concentration of nutrients which influence their proliferation and differentiation in comparison to the gradient pattern observed in 3D

environment [42]. We also postulate that the porous structure of scECMh (Figure 4C) facilitated greater proliferation rate in 3D environment compared to bECMh and dECMh.

A slight expression of some neural lineage markers by non-differentiated SCAP, attributed to their neural crest origin, was reported previously [43]. When SCAP were embedded into scECMh, there was a remarkable expression of key neural lineage markers on day 7 and day 14 (Figure 7). We hypothesise that the potential neurotrophic factors as well as proteoglycans embedded within scECMh have induced a neural-like phenotype. ECM scaffolds derived from CNS tissues have already been reported to induce neuronal cell differentiation of neuronal progenitor cells [9,20,23]. Furthermore, decellularisation using peracetic acid might have resulted in a higher concentration of FGF-2 as well as *sGAG* [44], which in turn enhanced the gene expression of neuronal lineage markers in scECMh. On day 14, SCAP embedded in bECMh also showed an expression of neural lineage genes. We hypothesise that the by-products of ECM degradation including soluble biomolecules in conjunction with scaffold elasticity may influence SCAP differentiation towards neural phenotype.

5 Conclusion

Solubilised forms of decellularised ECM from spinal cord, dentine and bone tissues were prepared by a combination of enzymatic and chemical processes and induced to form hydrogels. These acellular ECM hydrogels had discrete structural, mechanical and biological characteristics. Human stem cells from apical papilla exhibited a strong positive response to scECMh by proliferating within and on the hydrogel and by expressing neural genes; substantiating the influence of neurotrophic factors present in decellularized spinal cord. SCAP exhibited a greater proliferation rate in 2D in dECMh, compared to bECMh and scECMh, however no neuronal differentiation occurred. Neuronal lineage markers were expressed by SCAP when cultured with bECMh and it is hypothesized that the hydrogel mechanical properties combined with active biomolecules provided the stimulus for this behaviour. The results of the present study show that decellularised ECM hydrogels facilitate SCAP viability and proliferation. However, ECM hydrogels from site-specific tissues demonstrated are more likely to facilitate optimal stem cell behaviour for constructive spinal cord regeneration.

Acknowledgements

The authors would like to thank Dr Christopher Medberry and Professor Stephen Badylak for assistance with preparation of the spinal cord ECM. The authors also would like to thank MICA - Université Catholique de Louvain platform for Scanning Electron Microscope facility. Aiswarya Viswanath is supported by NanoFar "European Doctorate in Nanomedicine" EMJD programme funded by EACEA. This work is supported by grants from the Université Catholique de Louvain (F.S.R), Fonds National de la Recherché Scientifique (F.R.S.-FNRS). A. des Rieux is a F.R.S.-FNRS Research Associate and J. Vanacker is a F.R.S.-FNRS Postdoctoral Researcher. J. Leprince is supported by la Fondation Saint Luc.

References

1. McCreedy DA, Sakiyama-Elbert SE. Combination therapies in the CNS: engineering the environment. Neurosci Lett 2012;519(2):115-21.
2. Tator CH. Review of treatment trials in human spinal cord injury: issues, difficulties, and recommendations. Neurosurgery 2006;59(5):957-82; discussion 982-7.
3. Mothe AJ, Tator CH. Advances in stem cell therapy for spinal cord injury. J Clin Invest 2012;122(11):3824-34.
4. De Berdt P, Vanacker J, Ucakar B, Elens L, Diogenes A, Leprince JG, Deumens R, des Rieux A. Dental Apical Papilla as Therapy for Spinal Cord Injury. J Dent Res 2015;94(11):1575-81.
5. Huang GT-J, Gronthos S, Shi S. Mesenchymal Stem Cells Derived from Dental Tissues vs. Those from Other Sources: Their Biology and Role in Regenerative Medicine. Journal of Dental Research 2009;88(9):792-806.
6. Sakai K, Yamamoto A, Matsubara K, Nakamura S, Naruse M, Yamagata M, Sakamoto K, Tauchi R, Wakao N, Imagama S and others. Human dental pulp-derived stem cells promote locomotor recovery after complete transection of the rat spinal cord by multiple neuro-regenerative mechanisms. J Clin Invest 2012;122(1):80-90.
7. Martens W, Bronckaers A, Politis C, Jacobs R, Lambrichts I. Dental stem cells and their promising role in neural regeneration: an update. Clin Oral Investig 2013;17(9):1969-83.

8. Sonoyama W, Liu Y, Yamaza T, Tuan RS, Wang S, Shi S, Huang GT. Characterization of the apical papilla and its residing stem cells from human immature permanent teeth: a pilot study. J Endod 2008;34(2):166-71.

9. Crapo PM, Tottey S, Slivka PF, Badylak SF. Effects of biologic scaffolds on human stem cells and implications for CNS tissue engineering. Tissue Eng Part A 2014;20(1-2):313-23.

10. Bible E, Dell'Acqua F, Solanky B, Balducci A, Crapo PM, Badylak SF, Ahrens ET, Modo M. Non-invasive imaging of transplanted human neural stem cells and ECM scaffold remodeling in the stroke-damaged rat brain by (19)F- and diffusion-MRI. Biomaterials 2012;33(10):2858-71.

11. Sicari BM, Dziki JL, Siu BF, Medberry CJ, Dearth CL, Badylak SF. The promotion of a constructive macrophage phenotype by solubilized extracellular matrix. Biomaterials 2014;35(30):8605-8612.

12. Wolf MT, Carruthers CA, Dearth CL, Crapo PM, Huber A, Burnsed OA, Londono R, Johnson SA, Daly KA, Stahl EC and others. Polypropylene surgical mesh coated with extracellular matrix mitigates the host foreign body response. J Biomed Mater Res A 2014;102(1):234-46.

13. Singelyn JM, Sundaramurthy P, Johnson TD, Schup-Magoffin PJ, Hu DP, Faulk DM, Wang J, Mayle KM, Bartels K, Salvatore M and others. Catheter-deliverable hydrogel derived from decellularized ventricular extracellular matrix increases endogenous cardiomyocytes and preserves cardiac function post-myocardial infarction. J Am Coll Cardiol 2012;59(8):751-63.

14. Wang RM, Christman KL. Decellularized myocardial matrix hydrogels: In basic research and preclinical studies. Adv Drug Deliv Rev 2015.

15. Ballios BG, Cooke MJ, Donaldson L, Coles BL, Morshead CM, van der Kooy D, Shoichet MS. A Hyaluronan-Based Injectable Hydrogel Improves the Survival and Integration of Stem Cell Progeny following Transplantation. Stem Cell Reports 2015;4(6):1031-45.

16. DeQuach JA, Yuan SH, Goldstein LS, Christman KL. Decellularized porcine brain matrix for cell culture and tissue engineering scaffolds. Tissue Eng Part A 2011;17(21-22):2583-92.

17. Sellaro TL, Ranade A, Faulk DM, McCabe GP, Dorko K, Badylak SF, Strom SC. Maintenance of Human Hepatocyte Function In Vitro by Liver-Derived Extracellular Matrix Gels. Tissue Engineering Part A 2010;16(3):1075-1082.

18. Sellaro TL, Ravindra AK, Stolz DB, Badylak SF. Maintenance of hepatic sinusoidal endothelial cell phenotype in vitro using organ-specific extracellular matrix scaffolds. Tissue Eng 2007;13(9):2301-10.

19. Sawkins MJ, Bowen W, Dhadda P, Markides H, Sidney LE, Taylor AJ, Rose FR, Badylak SF, Shakesheff KM, White LJ. Hydrogels derived from demineralized and decellularized bone extracellular matrix. Acta Biomater 2013;9(8):7865-73.

20. Medberry CJ, Crapo PM, Siu BF, Carruthers CA, Wolf MT, Nagarkar SP, Agrawal V, Jones KE, Kelly J, Johnson SA and others. Hydrogels derived from central nervous system extracellular matrix. Biomaterials 2013;34(4):1033-40.

21. Bazos P, Magne P. Bio-emulation: biomimetically emulating nature utilizing a histo-anatomic approach; structural analysis. Eur J Esthet Dent 2011;6(1):8-19.

22. Hong Y, Huber A, Takanari K, Amoroso NJ, Hashizume R, Badylak SF, Wagner WR. Mechanical properties and in vivo behavior of a biodegradable synthetic polymer microfiber-extracellular matrix hydrogel biohybrid scaffold. Biomaterials 2011;32(13):3387-94.

23. Crapo PM, Medberry CJ, Reing JE, Tottey S, van der Merwe Y, Jones KE, Badylak SF. Biologic scaffolds composed of central nervous system extracellular matrix. Biomaterials 2012;33(13):3539-3547.

24. Woessner JF, Jr. The determination of hydroxyproline in tissue and protein samples containing small proportions of this imino acid. Arch Biochem Biophys 1961;93:440-7.

25. Farndale RW, Sayers CA, Barrett AJ. A Direct Spectrophotometric Micro-Assay for Sulfated Glycosaminoglycans in Cartilage Cultures. Connective Tissue Research 1982;9(4):247-248.

26. Wolf MT, Daly KA, Brennan-Pierce EP, Johnson SA, Carruthers CA, D'Amore A, Nagarkar SP, Velankar SS, Badylak SF. A hydrogel derived from decellularized dermal extracellular matrix. Biomaterials 2012;33(29):7028-38.

27. Ruparel NB, de Almeida JF, Henry MA, Diogenes A. Characterization of a stem cell of apical papilla cell line: effect of passage on cellular phenotype. J Endod 2013;39(3):357-63.

28. Crapo PM, Gilbert TW, Badylak SF. An overview of tissue and whole organ decellularization processes. Biomaterials 2011;32(12):3233-3243.

29. Badylak SF, Gilbert TW. Immune response to biologic scaffold materials. Seminars in Immunology 2008;20(2):109-116.

30. Engfeldt B, Hjerpe A. Glycosaminoglycans of dentine and predentine. Calcif Tissue Res 1972;10(2):152-9.

31. Liu Z, Masuko S, Solakyildirim K, Pu D, Linhardt RJ, Zhang F. Glycosaminoglycans of the porcine central nervous system. Biochemistry 2010;49(45):9839-47.

32. Stuart K, Panitch A. Influence of chondroitin sulfate on collagen gel structure and mechanical properties at physiologically relevant levels. Biopolymers 2008;89(10):841-51.

33. Weidner N, Grill RJ, Tuszynski MH. Elimination of basal lamina and the collagen "scar" after spinal cord injury fails to augment corticospinal tract regeneration. Exp Neurol 1999;160(1):40-50.

34. Clarke B. Normal bone anatomy and physiology. Clin J Am Soc Nephrol 2008;3 Suppl 3:S131-9.

35. Burnside ER, Bradbury EJ. Manipulating the extracellular matrix and its role in brain and spinal cord plasticity and repair. Neuropathol Appl Neurobiol 2014;40(1):26-59.

36. Black LD, Allen PG, Morris SM, Stone PJ, Suki B. Mechanical and failure properties of extracellular matrix sheets as a function of structural protein composition. Biophys J 2008;94(5):1916-29.

37. Marinkovic M, Block TJ, Rakian R, Li Q, Wang E, Reilly MA, Dean DD, Chen XD. One size does not fit all: developing a cell-specific niche for in vitro study of cell behavior. Matrix Biol 2016;52-54:426-41.

38. Engler AJ, Sen S, Sweeney HL, Discher DE. Matrix elasticity directs stem cell lineage specification. Cell 2006;126(4):677-89.

39. Tukmachev D, Forostyak S, Koci Z, Zaviskova K, Vackova I, Vyborny K, Sandvig I, Sandvig A, Medberry CJ, Badylak SF and others. Injectable Extracellular Matrix Hydrogels as Scaffolds for Spinal Cord Injury Repair. Tissue Eng Part A 2016;22(3-4):306-17.

40. Faulk DM, Carruthers CA, Warner HJ, Kramer CR, Reing JE, Zhang L, D'Amore A, Badylak SF. The effect of detergents on the basement membrane complex of a biologic scaffold material. Acta Biomater 2014;10(1):183-93.

41. Walters NJ, Gentleman E. Evolving insights in cell-matrix interactions: elucidating how non-soluble properties of the extracellular niche direct stem cell fate. Acta Biomater 2015;11:3-16.

42. Tibbitt MW, Anseth KS. Hydrogels as extracellular matrix mimics for 3D cell culture. Biotechnol Bioeng 2009;103(4):655-63.

43. Germain L, De Berdt P, Vanacker J, Leprince J, Diogenes A, Jacobs D, Vandermeulen G, Bouzin C, Préat V, Dupont-Gillain C and others. Fibrin hydrogels to deliver dental stem cells of the apical papilla for regenerative medicine. Regenerative Medicine 2015;10(2):153-167.

44. Hodde J, Janis A, Ernst D, Zopf D, Sherman D, Johnson C. Effects of sterilization on an extracellular matrix scaffold: part I. Composition and matrix architecture. J Mater Sci Mater Med 2007;18(4):537-43.

Tables and Figures

Table 1: Human genes and primers used for RT-PCR analysis

Symbol	***Gene name***	***Primer Sequence (5'->3')***	***Amplicon length (bp)***
GAPDH	*GAPDH = Glyceraldehyde 3-phosphate dehydrogenase*	F : GATCAACTCACCGCCAACA R : CCAGCGACTCAATCTTCCTC	452
SNAIL	*Zinc finger protein SNAI1*	F : CTAGGCCCTGGCTGCTACAA R :CATCTGAGTGGGTCTGGAGGT	129
BIII Tubulin		F : GGGCCTTTGGACATCTCTTC R : GGATACTCCTCACGCACCTT	244
PDGFRa	*Platelet-Derived Growth Factor Receptor, Alpha Polypeptide*	F : AGCTTGAAGGCAGGCACA R :GCGACAAGGTATAATGGCAG A	122
VEGFA	*Vascular endothelial growth factor A*	F : CATCTTCAAGCCATCCTGTG R : CAACGCGAGTCTGTGTTTT	303,357, 375,426
GDNF	*Glial cell derived neurotrophic factor*	F : CAGACATCTGATCCCCTTCC R : GCTGGGGTTTGTCACTGTTT	172

Table 2: Gelation kinetics for scECM, bECM and dECM hydrogels

Turbidity (Mean± SD)	**scECM (Mean± SD)**	**bECM (Mean± SD)**	**dECM (Mean± SD)**
Lag phase (t_{lag}: min)	11.998 ± 1.90	11.25 ± 1.4	7.8 ± 1.55
50% gelation ($t_{½}$: min)	20.582 ± 2.42	21.06 ± 3.2	14.60 ± 1.24
95% gelation (t_{95}: min)	30.248 ± 2.91	36.00± 0.00	39.85 ± 3.34
Speed (S, min^{-1})	0.0738 ± 0.009	0.057 ± 0.003	0.035 ± 0.004

n=8, $p<0.05$

Table 3: Influence of ECM origin on hydrogel final moduli

Material	Storage modulus (*G'*, Pa)	Loss modulus (*G''*, Pa)
bECM (8mg/ml)	287.17 ± 8.43 [A]	42.61 ± 3.72 [A]
dECM (8mg/ml)	4.79 ± 0.33 [B]	0.56 ± 0.128 [B]
scECM (8mg/ml)	19.35 ± 1.16 [C]	2.40 ± 0.385 [C]

ECM not related by the same letter are significantly different (G' and G'' separately) ($p<0.05$; n=3).

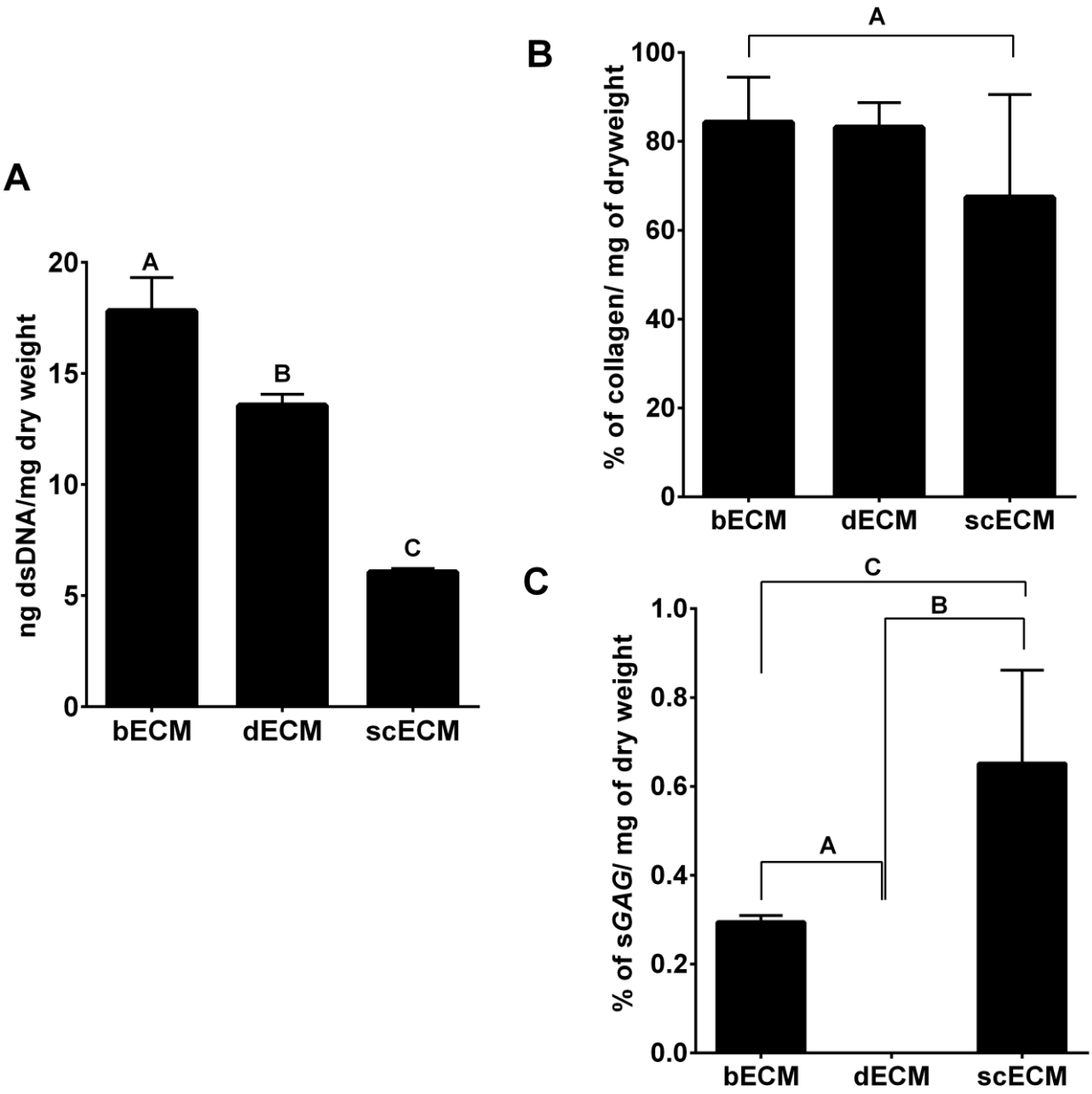

Figure 1: Influence of ECM origin on cellular, collagen and sGAG content.

(A) Efficiency of decellularisation was assessed by quantifying the amount of dsDNA/mg dry weight. B) Collagen content and (C) sGAG content of ECM scaffolds were evaluated by quantifying hydroxyproline and using the 1, 9 –Dimethyl methylene blue assay, respectively. Data is presented as Mean ± standard deviation (n=3). Conditions not linked by the same letter are significantly different ($p<0.05$).

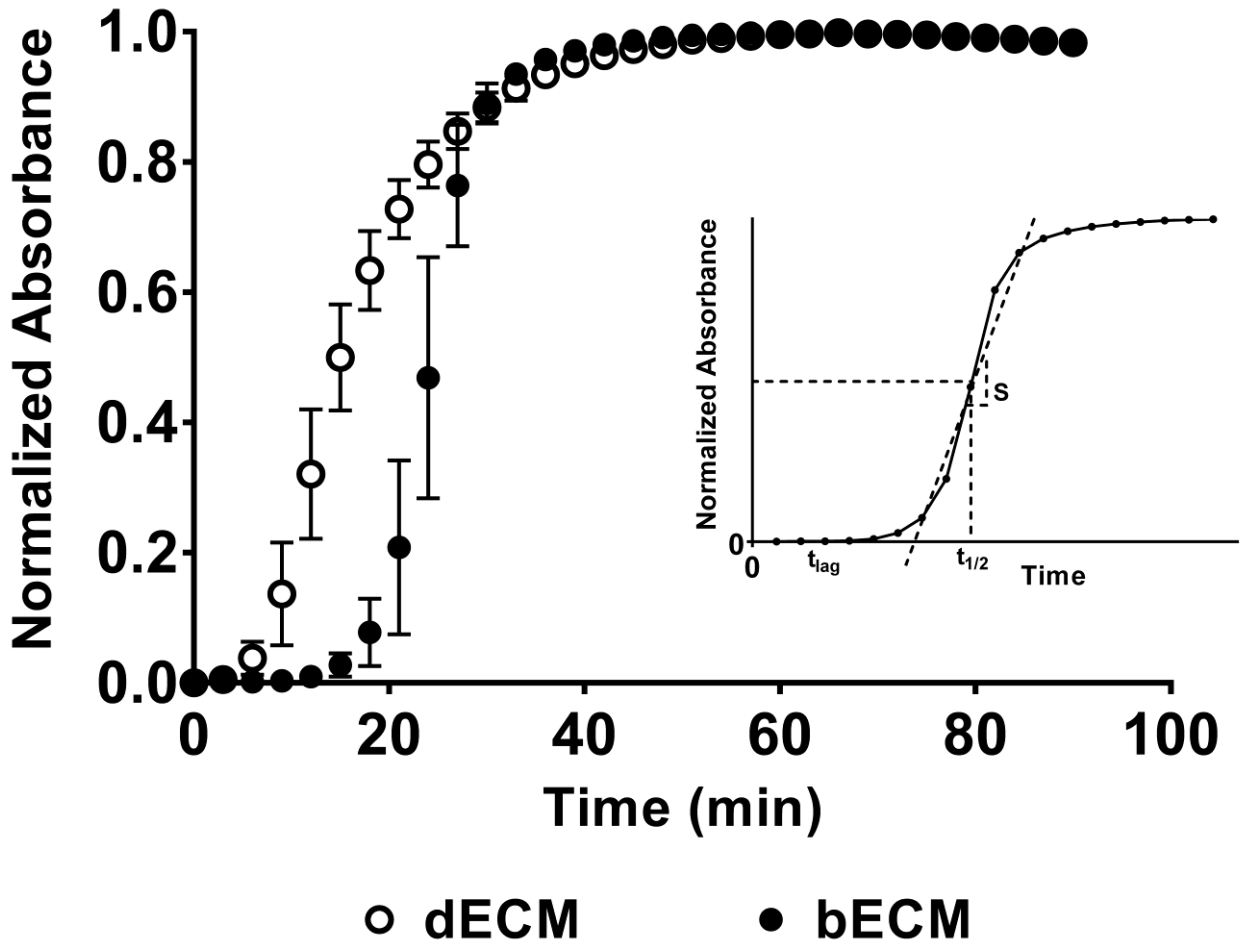

Figure 2: Turbidimetric gelation kinetics of scECM, bECM, and dECM scaffolds were compared at 8mg/ml concentrations. The neutralised pre-gel solution was added to a 96 well plate and gelation was induced at 370C. The absorbance was measured at 405nm and recorded at 3min intervals. The data was normalised between 0 (initial absorbance) and 1 (maximum absorbance). Data represents mean ± SD (n=8). Inset: diagrammatic representation of the parameters determined from normalised gelation kinetics.

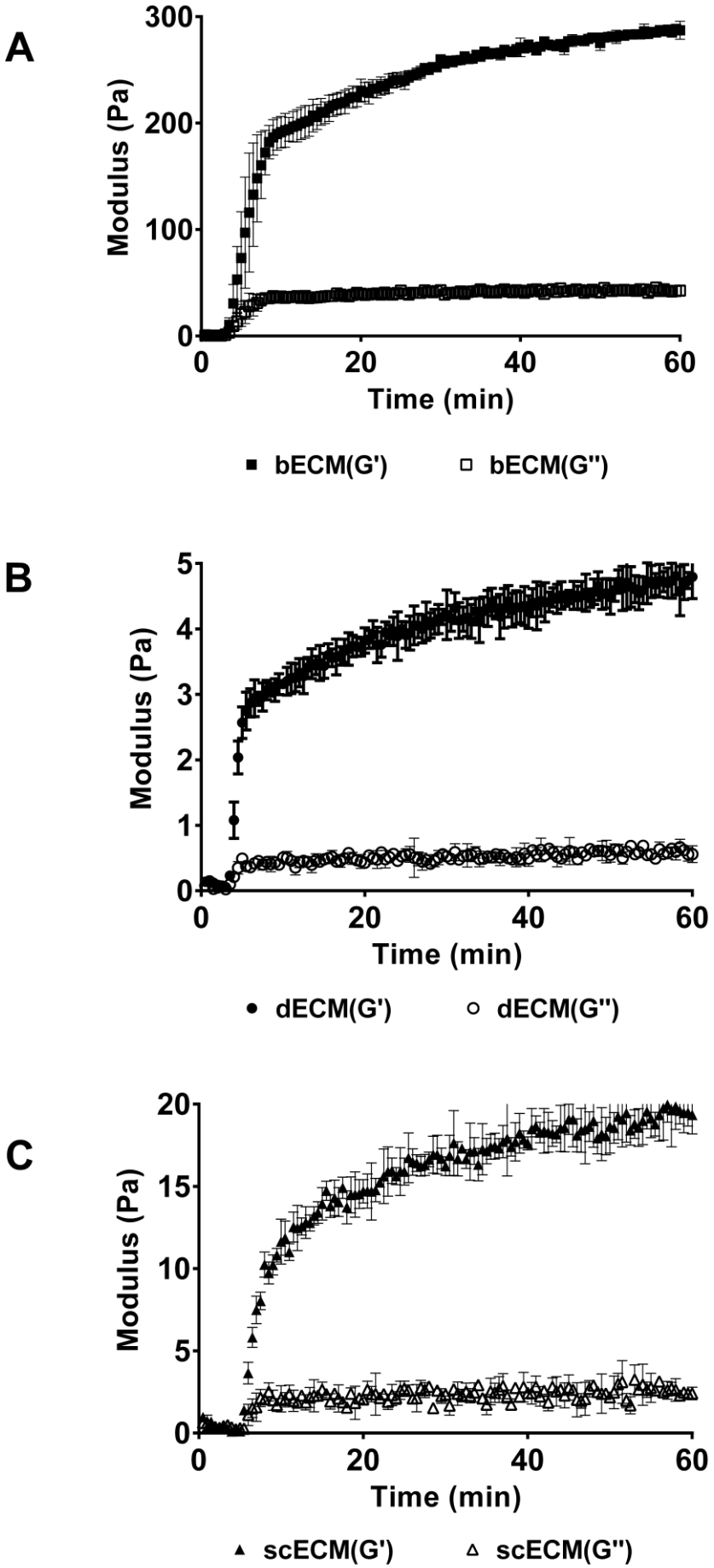
A
300
200
100
0
Modulus (Pa)
0
20
40
60
Time (min)
bECM(G')
bECM(G'')
B
5
4
3
2
1
0
Modulus (Pa)
0
20
40
60
Time (min)
dECM(G')
dECM(G'')
C
20
15
10
5
0
Modulus (Pa)
0
20
40
60
Time (min)
scECM(G')
scECM(G'')

Figure 3: Influence of ECM origin on hydrogel mechanical properties.

Rheological properties of hydrogels were investigated by small amplitude oscillatory shear rheology. The storage (G′) and loss moduli (G″) were measured using a Kinexus Pro rotational rheometer and rSpace software (n=3).

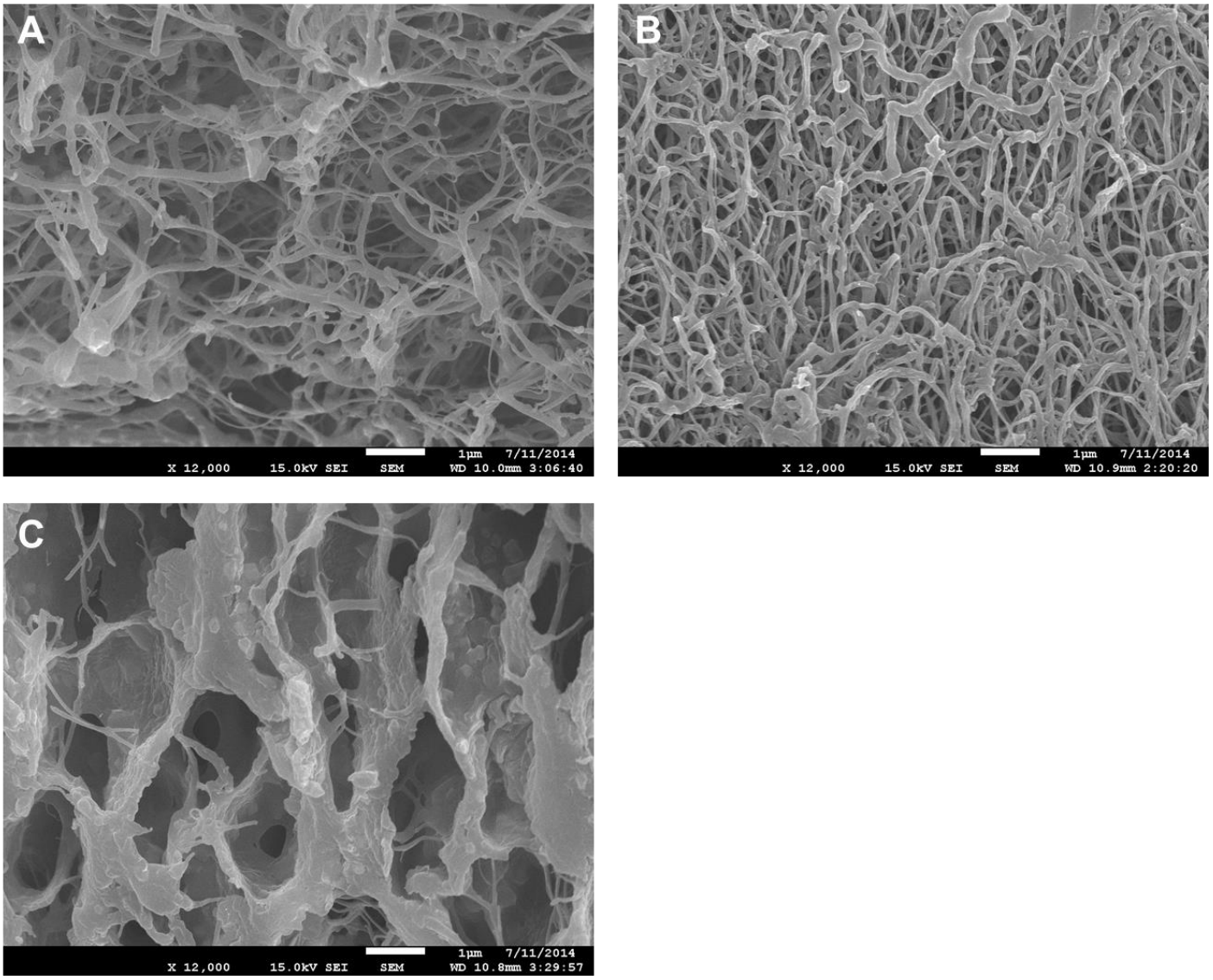

Figure 4: Influence of ECM origin on the hydrogel microstructure.

ECM hydrogels were formed and processed for SEM analysis, scale bar = 1 µm with (A) bECM, (B) dECM and (C) scECM hydrogels. Magnification: 12,000x.

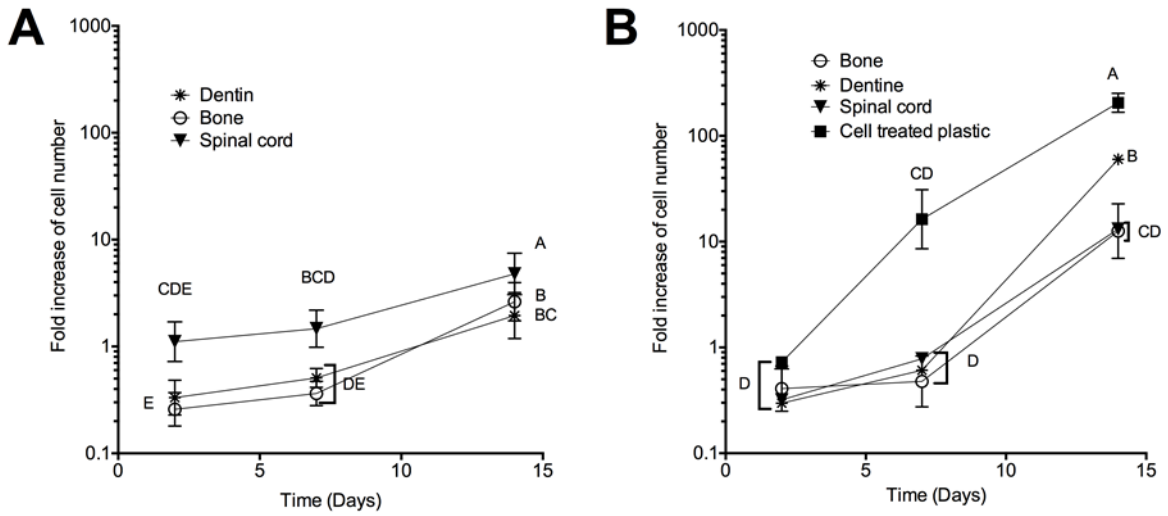

Figure 5: Influence of ECM origin on SCAP proliferation.

A- 500,000 SCAP/ml were incorporated in different ECM hydrogels and incubated at 37°C. Presto blue test was performed at different time points (2, 7 and 14 days). Fluorescence intensities were measured at 590 nm (n=6, N=3). B- Pre-gel solutions were allowed to gel at 37°C. Then 2000 SCAP were seeded on the ECM. After 2, 7 and 14 days, cell proliferation was analysed using a Presto Blue kit (n=6, N=3). As a positive control, the same amount of cells was seeded on tissue culture plastic. Conditions not related by the same letter are significantly different ($p < 0.05$).

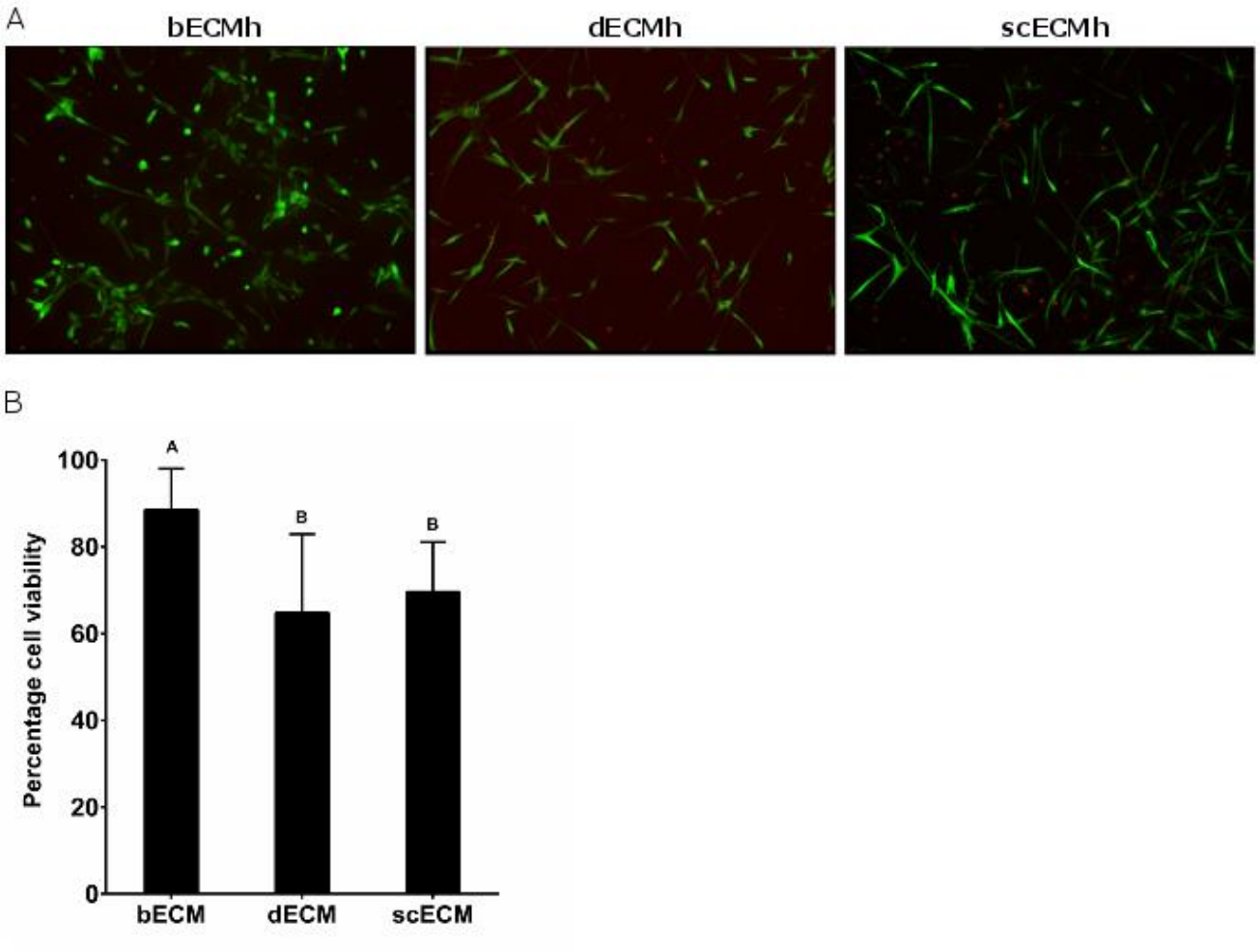

Figure 6: Influence of ECM origin on SCAP viability.

500,000 SCAP/ml were incorporated in different ECM hydrogels and incubated for 2 days. A Live/Dead assay was performed. Living and dead cells were observed by confocal microscopy (488 and 568 nm, respectively) (n=3, N=3). (A) Live cells were stained with Calcein (green) and dead cells were stained with ethidium homodimer-I (red). (B) The images were processed to quantify the number of live cells and dead cells using ImageJ (n = 3–5 acquisitions/sample). Conditions not related by the same letter are significantly different ($p < 0.05$).

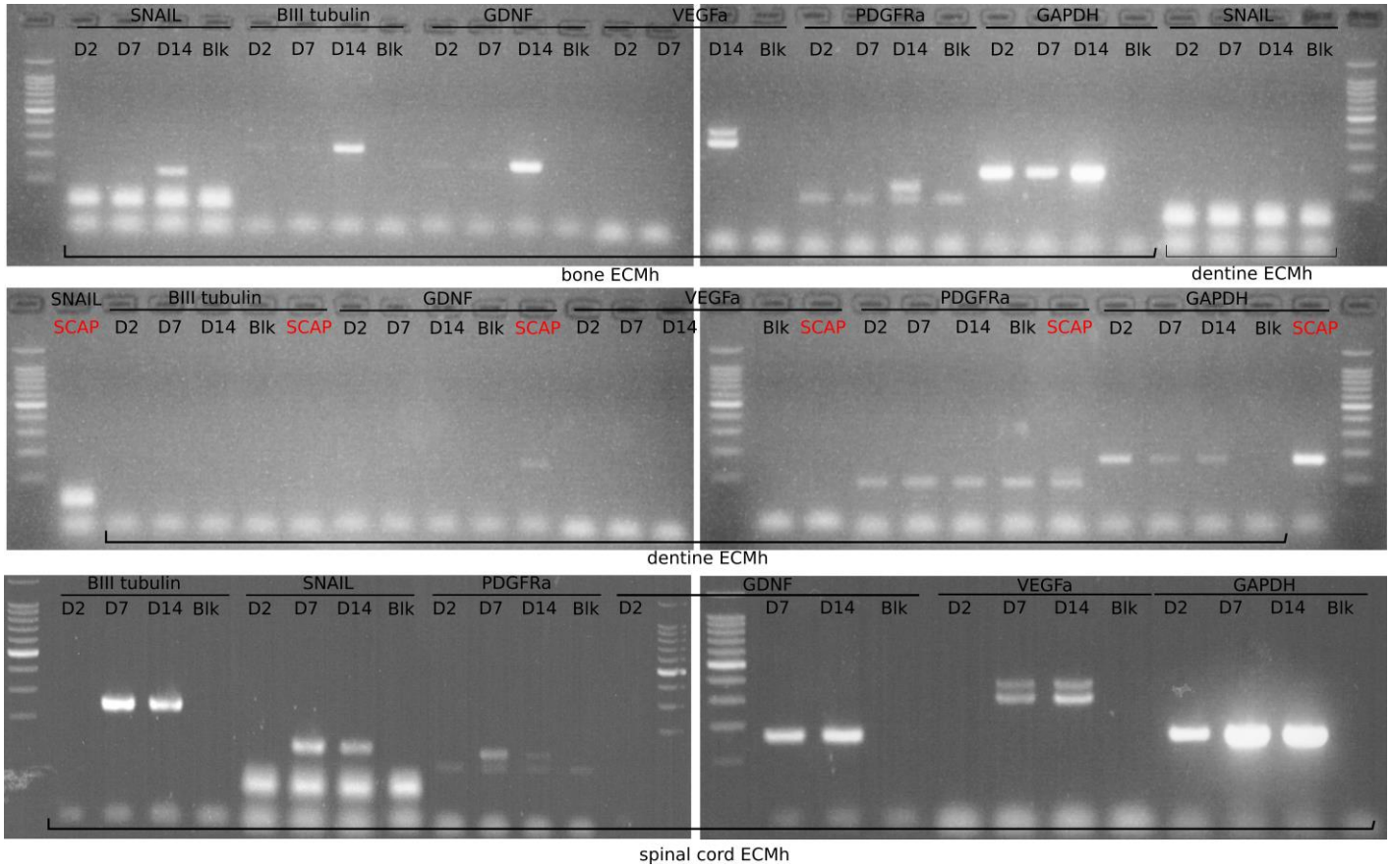

Figure 7: Influence of ECM origin on SCAP gene expression.

500,000 SCAP/ml were incorporated in different ECM hydrogels and incubated for 2, 7 and 14 days (D2, D7 and D14). mRNA were extracted and gene expression was analysed by RT-PCR (n=3, N=3). Blanks (Blk) were obtained by replacing mRNA by RNAse free water. Gene expression of SCAP grown in 2D without ECM hydrogel (SCAP) was also analysed.